Hindawi
Advances in Civil Engineering
Volume 2020, Article ID 8832522, 19 pages
https://doi.org/10.1155/2020/8832522

Research Article

Practical Hybrid Machine Learning Approach for Estimation of Ultimate Load of Elliptical Concrete-Filled Steel Tubular Columns under Axial Loading

Tien-Thinh Le [1,2]

[1]*Faculty of Mechanical Engineering and Mechatronics, Phenikaa University, Yen Nghia, Ha Dong, Hanoi 12116, Vietnam*
[2]*Phenikaa Research and Technology Institute (PRATI), A&A Green Phoenix Group JSC, No. 167 Hoang Ngan, Trung Hoa, Cau Giay, Hanoi 11313, Vietnam*

Correspondence should be addressed to Tien-Thinh Le; thinh.letien@phenikaa-uni.edu.vn

Received 11 June 2020; Revised 30 September 2020; Accepted 9 October 2020; Published 28 October 2020

Academic Editor: Murat Kankal

In this study, a hybrid machine learning (ML) technique was proposed to predict the bearing capacity of elliptical CFST columns under axial load. The proposed model was Adaptive Neurofuzzy Inference System (ANFIS) combined with Real Coded Genetic Algorithm (RCGA), denoted as RCGA-ANFIS. The evaluation of the model was performed using the coefficient of determination (R^2) and root mean square error (RMSE). The results showed that the RCGA-ANFIS ($R^2 = 0.974$) was more reliable and effective than conventional gradient descent (GD) technique ($R^2 = 0.952$). The accuracy of the present work was found superior to the results published in the literature ($R^2 = 0.776$ or 0.768) when predicting the load capacity of elliptical CFST columns. Finally, sensitivity analysis showed that the thickness of the steel tube and the minor axis length of the elliptical cross section were the most influential parameters. For practical application, a Graphical User Interface (GUI) was developed in MATLAB for researchers and engineers and to support the teaching and interpretation of the axial behavior of CFST columns.

1. Introduction

In recent decades, composite concrete-filled steel tubular (CFST) columns are considerably employed in the construction of infrastructures thanks to their excellent structural behavior [1]. These structural members exhibit many benefits than single material columns (i.e., concrete columns or hollow steel columns). These advantages could be listed as fire, axial capacity, and earthquake resistance [2, 3]. In practical engineering, various cross section geometries of CFST columns have been considered, such as circular [4], square [5], or rectangular cross sections [6]. Recently, the elliptical cross section was adopted in several works [3, 7, 8]. Indeed, the use of elliptical CFST columns has gained attention from the scientific community and applied engineering as it provides specific advantages compared to other cross sections of CFST, including a better strength and rigidity as well as fire resistance [9]. Due to its reasonable distribution of the major-minor axis, elliptical CFST column exhibits a better architectural aesthetic appearance and a small fluid resistance coefficient [10, 11]. Moreover, the prevention of local buckling in the elliptical CFST columns could be well-established thanks to the concrete core [12, 13]. The elliptical section possesses aesthetic qualities along with more effective bending resistance when compared to circular section due to having different second moments of area around its principal axes [14]. Therefore, analyzing the structural behavior, especially the ultimate load of elliptical CFST columns, is essential to facilitate the use in civil engineering structures.

However, there are currently no standards or codes in any countries for assessing the load-carrying capacity of elliptical CFST columns [15]. Besides, there were several empirical formulations in the available literature such as Liu and Zha 2011 [16] and Shen et al. [17] for predicting the ultimate load of elliptical CFST members. However,

these equations were derived using assumptions and experimental observations, which led to a simplification of the prediction model. Consequently, the application of these models could not be extended to other results. All these limit the application of elliptical CFST columns in engineering practice. Although previous studies provided significant contributions to the progress in modeling and prediction of axial behavior of CFST members, a more robust and efficient model should be developed to reduce the cost and time consumed in experiments and field works.

Recently, machine learning (ML) approaches have been employed in various mechanical and civil engineering applications [18, 19], particularly for structural members under compression [20, 21]. As an example, Sarir et al. [22] proposed a tree-based and whale optimization model for predicting the load-bearing capacity of circular CFST members. Besides, Ahmadi et al. [23, 24] applied an artificial neural network for predicting the axial capacity of circular CFST short columns. In another work, Tran et al. [25] developed a neural network-based model for predicting the load-bearing capacity of square CFST columns. The obtained results in the literature demonstrated that ML methods have a very promising potential for predicting the mechanical behavior of structural elements. Despite the importance of elliptical CFST columns, most ML-based studies focused on circular and square cross sections [22, 26, 27]. Therefore, more investigations should be carried out to assess the potential applications of ML-based models for studying the axial behavior of elliptical CFST columns.

Therefore, the primary objective of the present work was to develop an ML-based model to predict the ultimate load of elliptical CFST columns under axial loading. For this purpose, a hybrid ML model, namely Adaptive Neurofuzzy Inference System (ANFIS) combined with Real Coded Genetic Algorithm (RCGA), was developed. The RCGA was chosen because of its higher optimization capability than the conventional gradient descent (GD) technique, as highlighted in this study. As the present work mainly focused on elliptical CFST columns, the input data included the length of the column, the major and minor axis lengths of the elliptical cross section, the thickness of the steel tube, and the mechanical properties of steel and concrete (i.e., yield strength and compressive strength, respectively). In order to train and validate the developed hybrid ML model, statistical quality assessments such as coefficient of determination (R^2) and root mean squared error (RMSE) were employed. Monte Carlo simulations were also carried out in order to estimate the robustness of the proposed ML model. A sensitivity analysis was conducted to investigate the influence of input variables on the prediction results. The prediction capacity of the RCGA-ANFIS model was also compared with existing equations in the literature for estimating the ultimate load of elliptical CFST columns. Finally, a Graphical User Interface (GUI) based on the developed ML model was provided, aiming at quick and efficient estimation of the ultimate load of elliptical CFST columns.

2. Materials and Methods

2.1. Database. In this work, a database was constructed by extracting available datasets from experimental research of Uenaka [28], Yang et al. [29], Liu et al. [30], Ren et al. [12], Dai et al. [31], Jamaluddin et al. [32], Yang et al. [33], McCann et al. [34], and Zhao and Packer [35]. From these investigations, a total number of 94 configurations were collected and summarized (Table 1), including the number of data points and proportion (in %). As revealed in the literature, the experimental procedure was conducted following the steps below:

(i) Design of specimens
(ii) Manufacturing of steel tube
(iii) Manufacturing of concrete core
(iv) Assembly of composite columns
(v) Loading and measurement (see Figure 1 for a schematic description of the test as well as geometrical parameters of the members)

In terms of the experimental studies, various geometrical parameters, as well as mechanical properties of the constituent materials, were considered in order to test the failure of elliptical CFST columns under axial compression. For that reason, the input parameters of the problem regarding the geometry were the length of the column (denoted by L), the major axis length of the elliptical cross section (denoted by D), the minor axis length of the elliptical cross section (denoted by d), and the thickness of the steel tube (denoted by δ). Regarding the mechanical properties of constituent materials, the yield strength of the steel tube (denoted by f_y) and the compressive strength of the filled concrete (denoted by f'_c) were considered. The ultimate load of the column under axial compression was the output of the problem, denoted by Q_n. A primarily statistical analysis of the database is indicated in Table 2, including the min, average, max, standard deviation (StD), and coefficient of variation (CV) values of all variables. It should be noticed that several statistical correlation techniques such as Principal Component Analysis [36] were applied, and no significant correlations were found in the input space. This confirmed that, for the prediction problem, all input parameters in this study were independent, and the selection of inputs was relevant. Finally, all data were scaled into the range of [−1, 1] in order to minimize numerical bias in the training phase.

2.2. Methods Used

2.2.1. Adaptive Neurofuzzy Inference System (ANFIS). The Adaptive Neurofuzzy Inference System, referred to as ANFIS, is an ML model constructed from the combination between a set of fuzzy if-then rules and the fuzzy inference systems through an adaptive network [37, 38]. The main idea of ANFIS is to construct a set of fuzzy if-then rules, including suitable membership functions to create the stipulated output and input variables [39, 40]. Supposing that the ANFIS model has two input variables such as X and Y and

Table 1: Organization of database.

Source of data	Number of data points	Proportion of data (%)
Uenaka [28]	19	20.2
Yang et al. [29]	2	2.1
Liu et al. [30]	18	19.1
Ren et al. [12]	6	6.4
Dai et al. [31]	13	13.8
Jamaluddin et al. [32]	17	18.1
Yang et al. [33]	9	9.6
McCann et al. [34]	2	2.1
Zhao and Packer [35]	8	8.5
Total	94	100

one output variable such as Z, we apply the following Takagi and Sugeno's if-then rules [41, 42]:

$$\begin{aligned} &\text{If } X \text{ is } A_1 \text{ and } Y \text{ is } B_1, \quad \text{then } Z_1 = a_1X + b_1Y + c_1 \text{ (rule 1)};\\ &\text{If } X \text{ is } A_2 \text{ and } Y \text{ is } B_2, \quad \text{then } Z_2 = a_2X + b_2Y + c_2 \text{ (rule 2)}. \end{aligned} \tag{1}$$

Here, A and B are linguistic labels characterized by appropriate membership functions, and a, b, and c are the linear output parameters.

Consider the above ANFIS model with two input variables X and Y. Its structure can be divided into five main layers as follows [43]:

Layer 1: each node in this layer corresponds to a node function, which can be chosen to be bell-shaped with a minimum value equal to 0 and a maximum value equal to 1, for example, the Gaussian function, such that

$$\mu A_i(x) = \exp\left[-\left(\frac{x - a_i}{b_i}\right)^2\right], \tag{2}$$

where x is problem input and a_i, b_i are input parameters.

In fact, any continuous and differentiable functions can be chosen for the nodes in this layer.

Layer 2: each node in this layer is a node function that multiplies the incoming inputs and sends the results to the next layer:

$$w_i = \mu C_i^1(x_1) \times \mu C_i^2(x_2) \times \cdots \times \mu C_i^n(x_n). \tag{3}$$

Layer 3: each node in this layer computes the ratio between the ith rule's firing strength and the sum of all rules' firing strength:

$$\overline{w}_i = \frac{w_i}{\sum_{k=1}^{n} w_k}. \tag{4}$$

Layer 4: each node in this layer is a node function chosen such that

$$f_i = \overline{w}_i\left(c_0 + \sum_{k=1}^{n} c_k X_k\right). \tag{5}$$

Layer 5: the circle node in this layer calculates the sum of all incoming results and exports as the overall output

$$\text{Overall ouput} = \sum_i \overline{w}_i f_i. \tag{6}$$

The training algorithm uses a combination of the least-squares and backpropagation gradient descent methods to model the training dataset [44].

2.2.2. Real Coded Genetic Optimization Algorithm. Real Coded Genetic Algorithm, referred to as RCGA, is a metaheuristic optimization technique which is inspired by the principles of biological evolution. The basic idea of RCGA is to move a population of chromosomes, which are composed of strings of ones and zeros (or genes), to a new one that performs better than the old one [45]. There are two primary operations in RCGA, which are crossover and mutation [46, 47]. Crossover is a phase where the chromosomes in the population randomly share their features. This is the most significant operation in the RCGA, as more powerful offspring are created taking useful features from their parent's genes. Mutation is a process that is operated within each offspring, meaning that some of the bits in the bit string can be flipped. The main objective of the mutation process is to maintain the diversity of the population after new offspring are created from crossover [48].

The RCGA can be divided into five main steps as follows [48, 49]:

(i) Initial population. In this step, a set of chromosomes called population is defined. Each individual of the population corresponds to a solution of the considered problem. Each chromosome is formed by joining genes into a string. Typically, chromosomes are composed of strings of ones and zeros.

(ii) Fitness function. In this step, the fitness score of each individual in the population is calculated. It defines how to fit the chromosome or the ability of that chromosome to compete with others. A higher fitness score means that the individual is more likely to be reproduced.

(iii) Selection. In this step, the chromosomes with the highest values of fitness score will be selected in order to share their features in the next step.

(iv) Crossover. In this step, the crossover process will be operated on the most fitting chromosomes. Their genes are randomly exchanged to create new offspring.

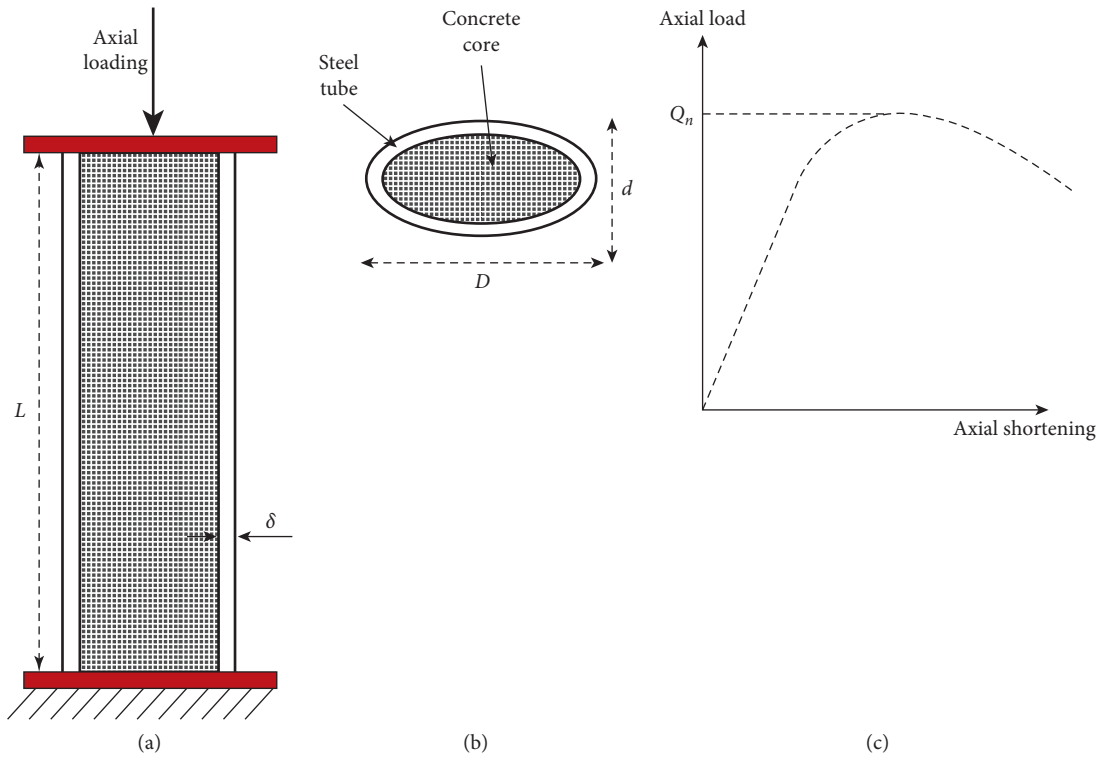

Figure 1: Schematization for (a) the CFST columns under axial loading, (b) the elliptical cross section, and (c) the load-axial shortening curve (a drawing based on experimental curves of Uenaka [28]).

Table 2: Initial statistical analysis of the database.

Parameter	Unit	Notation	Min	Average	Max	StD	CV (%)
Length of column	mm	L	160	991.86	3600	923.908	93.1
Major axis length of cross section	mm	D	136.5	177.281	318.5	35.986	20.3
Minor axis length of cross section	mm	d	63.1	93.693	155	21.466	22.9
Thickness of steel tube	mm	$\delta m1$	3.854	9.72	1.679	43.6	
Yield strength of steel tube	MPa	f_y	201	360.657	439.3	59.378	16.5
Compressive strength of concrete	MPa	f'_c	13.18	48.638	102.26	20.843	42.9
Ultimate load	kN	Q_n	413.3	1130.462	2607	484.164	42.8

(v) Mutation. In this step, the mutation process is done within each individual offspring to maintain the diversity of the population.

The algorithm is terminated when the model has converged, meaning that the newly created offspring are not different from the previous ones. In the literature, RCGA was used mainly in hybrid ML approaches [49]. For instance, Kim and Shin [50] used a hybrid approach based on neural networks and genetic algorithms for detecting temporal patterns, Le et al. [51] in steel structures applications, or Yan et al. [52] for engineering design problems. Finally, a complete review of the RCGA technique could be found in Lee [53].

2.2.3. Random Sampling Technique: Monte Carlo Method. The main idea of the Monte Carlo method is that the output is computed by repeating the sampling of variables randomly from the input space [54–56]. That way, (i) the Monte Carlo method is widely applied in order to propagate the variability of inputs on the output response; (ii) based on statistical analysis of output, several posttreatments such as robustness and/or sensitivity analyses could be thoroughly achieved [57] (see Figure 2 for a typical statistical problem using the Monte Carlo method). As shown in Figure 2, each input exhibits a probability distribution describing its variability. Due to the variabilities of input variables, the response also exhibits its statistical behaviors, which are necessary to be characterized [58]. The robustness of the model and/or sensitivity of input variables could then be deduced based on statistical analysis of output response [59–61].

Using Monte Carlo simulation, the bigger the number of realizations, the higher the reliability of the response archived. In this work, in order to optimize the number of Monte Carlo runs, a statistical estimator of convergence was applied, such as [62–65]

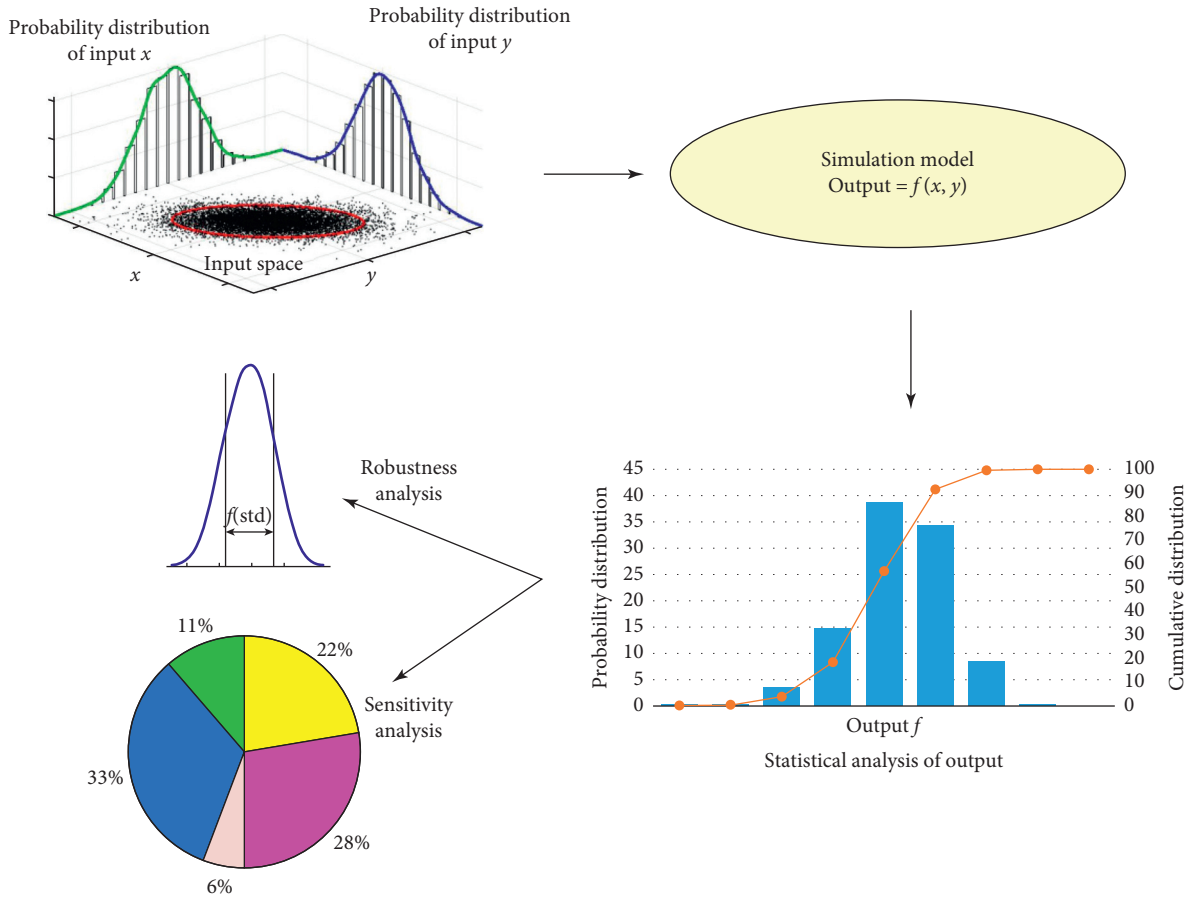

Figure 2: Monte Carlo simulation taking into account variability in the input space for robustness and sensitivity analysis.

$$N_{\mathrm{MC}} \mapsto I\left(N_{\mathrm{MC}}\right) = \frac{1}{\overline{W}} \frac{1}{N_{\mathrm{MC}}} \sum_{i=1}^{N_{\mathrm{MC}}} W_i, \tag{7}$$

where $\overline{W}$ is the mean of the considered variable W and N_{MC} is the number of Monte Carlo runs.

2.3. Quality Assessment Criteria. In the present work, statistical criteria, namely, the coefficient of determination (R^2) and Root Mean Squared Error (RMSE), have been used in order to validate and test the developed ML model. The R^2 allows us to identify the statistical relationship between two data points. This measurement of the linear correlation yields a value between 0 and 1 inclusively, where 0 is no correlation and 1 is total correlation. R^2 could be calculated using the following equation [66, 67]:

$$R^2 = \frac{\left(\sum_{k=1}^{N} \left(p_k - \overline{p}\right)\left(w_k - \overline{w}\right)\right)^2}{\sum_{k=1}^{N} \left(p_k - \overline{p}\right)^2 \sum_{k=1}^{N} \left(w_k - \overline{w}\right)^2}, \tag{8}$$

where N is the number of the observations, p_k and $\overline{p}$ are predicted and mean predicted values, and w_k and $\overline{w}$ are measured and mean measured values of ultimate load, respectively ($k = 1{:}\ N$). The formulation of RMSE is described by the following equation [68–70]:

$$\mathrm{RMSE} = \sqrt{\frac{1}{N} \sum_{k=1}^{N} \left(p_k - w_k\right)^2}. \tag{9}$$

Finally, the slope criterion is defined, such as the slope of the linear regression fit between predicted and observed vectors.

3. Results and Discussion

3.1. Optimization of ANFIS's Weight Parameters. In this section, the optimization of ANFIS's weight parameters is presented. Such optimization procedure was done using both conventional GD and advanced RCGA techniques, respectively, to identify the best training algorithm. Table 3 indicates the characteristics of ANFIS, including the type of membership function, the number of weights per membership function, and the number of membership functions per input as well as the number of nodes. It is seen that there were 190 consequent and antecedent ANFIS parameters to be optimized as ANFIS was generated using the c-means clustering algorithm for the considered six-dimensional input space [71, 72]. In this study, a maximum number of iterations of 1000 was employed as the stopping condition when optimizing. The cost function was selected as RMSE.

Table 3: Parameters of ANFIS and RCGA used in this study.

Parameter of ANFIS	Value	Parameter of RCGA	Value
Number of inputs	6	Population size	100
Number of outputs	1	Length of chromosome	190
Membership function	Gaussian	Fitness function	Linear ranking
Number of parameters per membership function	2	Crossover type	Random pair
Number of membership functions per input (rules)	10	Crossover probability	0.4
Number of nodes	149	Number of offsprings	12
Number of nonlinear parameters of the antecedent membership function	120	Mutation type	Random
Number of linear parameters of the consequent membership function	70	Mutation probability	0.7
Total number of parameters	190	Number of mutants	21
Cost function	RMSE	Mutation rate	0.15
		Selection function	Fitness proportionate selection

The parameters of RCGA during the training phase are also indicated in Table 3. Figures 3(a) and 3(c) present the evolution of RMSE during the optimization process, using GD and RCGA, respectively. The same illustration is presented in Figures 3(b) and 3(d), but for the evolution of R^2. It should be noticed that, in these figures, the value of RMSE (i.e., R^2) for training and testing data was also highlighted during the learning phase. It is seen that at least 600 iterations were needed for obtaining a convergence with respect to both RMSE and R^2. At the same time, the evolution of RMSE and R^2 is plotted using the testing data, which were totally new when applied. Such evolution exhibits efficiency during the training process; i.e., no overfitting or underfitting was observed.

The values of all quality assessment criteria at the end of the training process are indicated in Table 4, whereas the results in terms of regression plots and error distribution are shown in Figures 4(a)–4(c), respectively. As indicated in Table 4, using the training data, RCGA-ANFIS provided the highest value of R^2, which is 0.971, while the R^2 value of GD-ANFIS is 0.933. In terms of RMSE, RCGA-ANFIS yielded the smallest value, which is 70.379 kN, whereas the RMSE value of GD-ANFIS is 105.428 kN. In terms of linear fit, the RCGA-ANFIS model produced the highest value of slope (0.98) corresponding to a slope angle of 44.425°, while the slope value of GD-ANFIS was 0.937 corresponding to slope angle of 43.125°. Regarding error analyses, using the training data, the mean values are 1.409 and 0.972%, while the corresponding standard deviation values are 11.082 and 8.497% for GD-ANFIS and RCGA-ANFIS, respectively. It can be seen that the RCGA-ANFIS model yielded an error mean, which is the closest to zero and the smallest standard deviation value (see also Figure 4(c)). The application of the two ML models to the validating data is presented in the next section.

3.2. Validation of Model. The previously developed GD-ANFIS and RCGA-ANFIS models were applied to the validating data for validation. As a result, Figures 5(a) and 5(b) present regression graphs between actual and predicted ultimate load, whereas Figure 5(c)shows error distribution, respectively. All quantitative values of quality assessment criteria are indicated in Table 4. As indicated in Table 4, using the validating data, GD-ANFIS provided $R^2 = 0.952$, RMSE = 130.065 kN, $\text{Mean}_{\text{error}} = -0.456$ kN, $\text{StD}_{\text{error}} = 8.967$ kN, and slope = 0.920, whereas RCGA-ANFIS provided $R^2 = 0.974$, RMSE = 100.340 kN, $\text{Mean}_{\text{error}} = 2.541$ kN, $\text{StD}_{\text{error}} = 8.042$ kN, and slope = 1.019, respectively. The same remarks were obtained for the training data, RCGA-ANFIS yielded the best prediction performance. It could be stated that the RCGA-ANFIS model is validated because it performs well the prediction of ultimate load using the validating data. Thus, RCGA-ANFIS model was selected as the final prediction model for estimating the ultimate load of elliptical CFST columns.

3.3. Sensitivity Analysis. In this section, the influence of input variables on the prediction of column load-carrying capacity is presented. For this purpose, the probability distribution of each input was characterized by 11 levels of quantiles such as Q_0, Q_{10}, Q_{20}, Q_{30}, Q_{40}, Q_{50}, Q_{60}, Q_{70}, Q_{80}, Q_{90}, and Q_{100}. For a given input, a local influence index, denoted by θ (in %), was computed by the following equation:

$$\theta_q^k = \frac{\left|Q_q^k - Q_{\text{median}}^{\text{all}}\right|}{Q_{\text{median}}^{\text{all}}} \times 100, \tag{10}$$

where $Q_{\text{median}}^{\text{all}}$ is the output, the ultimate load when all inputs are equal to their Q_{50} values. Q_q^k is the output of the ML model when applying kth input at its qth levels (quantiles from 0 to 100 every 10, respectively) ($k = 1, \ldots, 6$ and $q = 1, \ldots, 11$). That way, the global influence index of the kth input, denoted by M^k, is calculated as follows:

$$M^k = \sum_{q=1}^{11} \theta_q^k. \tag{11}$$

Figures 6(a) and 6(b) present the global influence index of all inputs parameters using GD-ANFIS and RCGA-ANFIS, respectively (see the appendix for statistical convergence of Monte Carlo simulations). It could also be

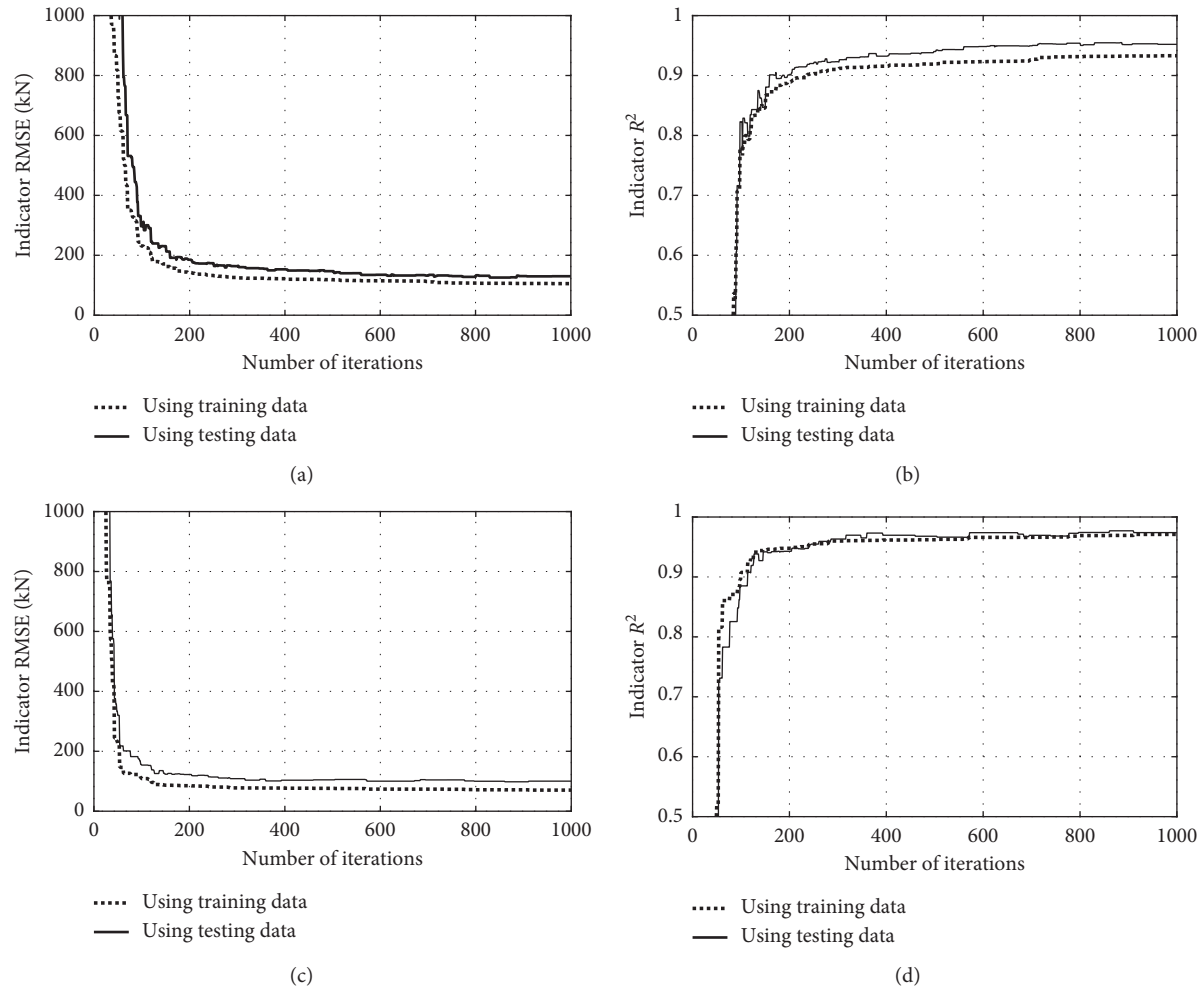

Figure 3: Evolution during optimization process for RMSE using (a) GD and (c) RCGA; for R^2 using (b) GD and (d) RCGA.

Table 4: Summary of prediction capability.

Data used	Model	R^2	RMSE	$\text{Mean}_{\text{error}}$ (%)	$\text{StD}_{\text{error}}$ (%)	Slope	Slope angle (°)
Training	GD-ANFIS	0.933	105.428	1.409	11.082	0.937	43.125
	RCGA-ANFIS	0.971	70.397	0.972	8.497	0.980	44.425
Testing	GD-ANFIS	0.952	130.065	−0.456	8.967	0.920	42.600
	RCGA-ANFIS	0.974	100.340	2.541	8.042	1.019	45.536

noticed that the bar graphs are reorganized in decreasing order of the mean value for all six input variables. All values are indicated in Table 5. It is clearly observed that all input variables affect the axial capacity of structural members considerably under axial compression from a minimum of 6.1% to a maximum of 22.5% on average. It is also seen that the axial capacity is in function of inputs under a nonlinear form (i.e., a linear equation could not join all mean values of sensitivity index). It is seen that there are at least four levels of influence ranking. Indeed, the two most important variables are d and δ, which exhibit more than 20% of influence each. Next, L and D could be classified in the second group, which exhibit about 18% of influence each. The third group contains the compressive strength of concrete, whereas the yield strength of steel has about 6% of influence and is in the last group. Last but not least, it is seen that the fluctuation of the influence index obtained by GD-ANFIS is higher than the ones obtained by RCGA-ANFIS. This points out that RCGA-ANFIS is more robust and efficient than GD-ANFIS, which confirms the higher performance of RCGA than GD, as identified in Section 3.2.

3.4. Comparison with Existing Models. In this section, the best prediction model, namely RCGA-ANFIS, is compared with existing models in the literature for the axial capacity of

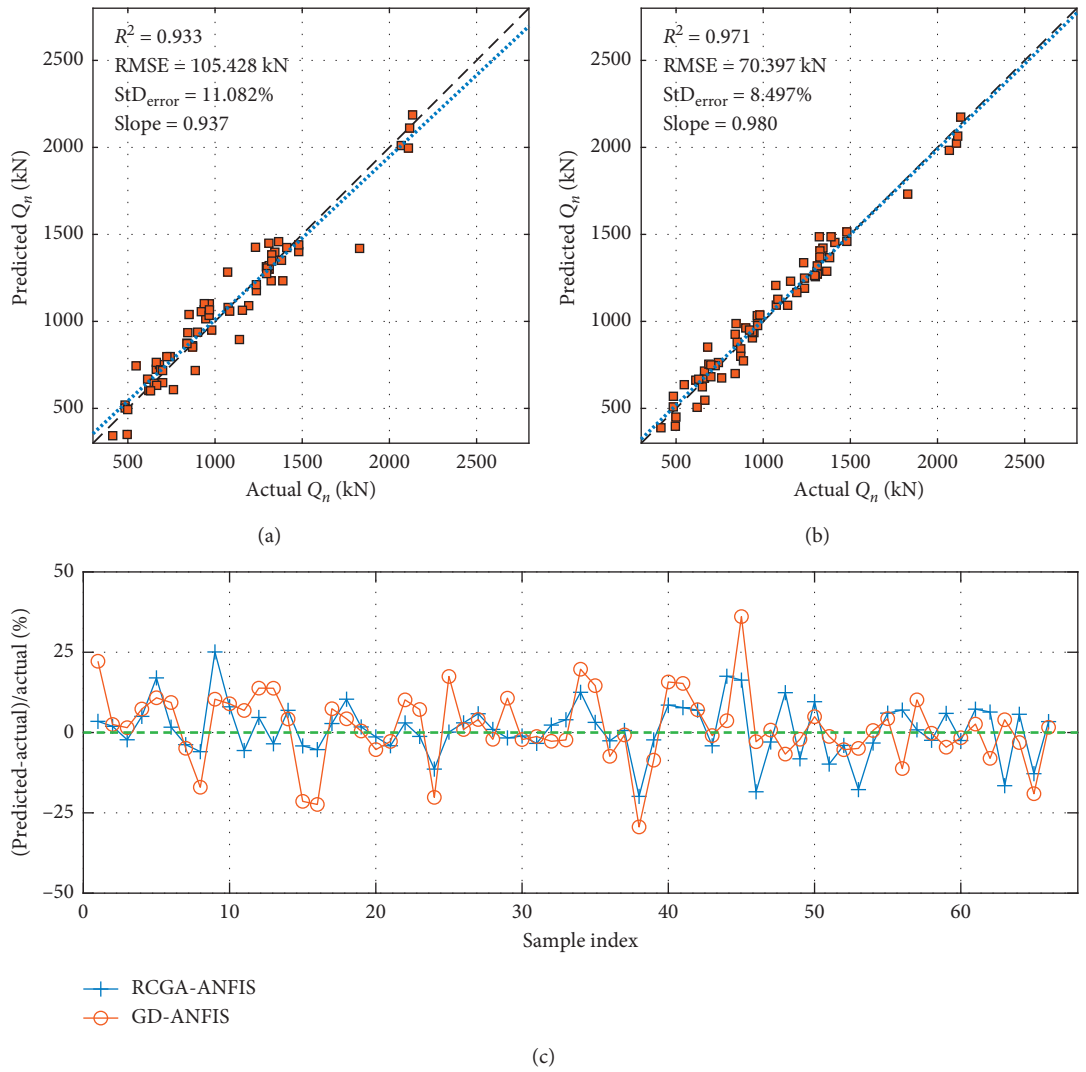

Figure 4: Results after training process for (a) using GD, (b) using RCGA, and (c) distribution of errors.

elliptical CFST columns. Liu and Zha [16] have proposed the following equation:

$$Q_n^{\text{Liu-2011}} = \frac{1 + 1.5\,(d/D)^{0.3}}{1 + (A_s/A_c)} \times \frac{A_s f_y}{A_c}, \tag{12}$$

where A_s and A_c are the cross-sectional area of the steel tubular and the concrete core, respectively. Another formula for predicting the axial capacity of elliptical CFST columns was developed by Shen et al. [17], such as

$$Q_n^{\text{Shen-2015}} = f_c'\,(A_s + A_c)\left[0.0075 \times \left(\frac{A_s f_y}{A_c f_c'}\right)^3 + 0.0624 \times \left(\frac{A_s f_y}{A_c f_c'}\right)^2 + 0.7080 \times \left(\frac{A_s f_y}{A_c f_c'}\right) + 1.3625\right]. \tag{13}$$

Figures 7(a)–7(c) present the regression graph between actual and predicted ultimate load, using Liu et al. 2011, Shen et al. 2015, and RCGA-ANFIS model, respectively. All performance indicators are also highlighted in Table 6. It is seen in Figure 7 and Table 6 that the RCGA-ANFIS model provided better performance than the literature, with respect

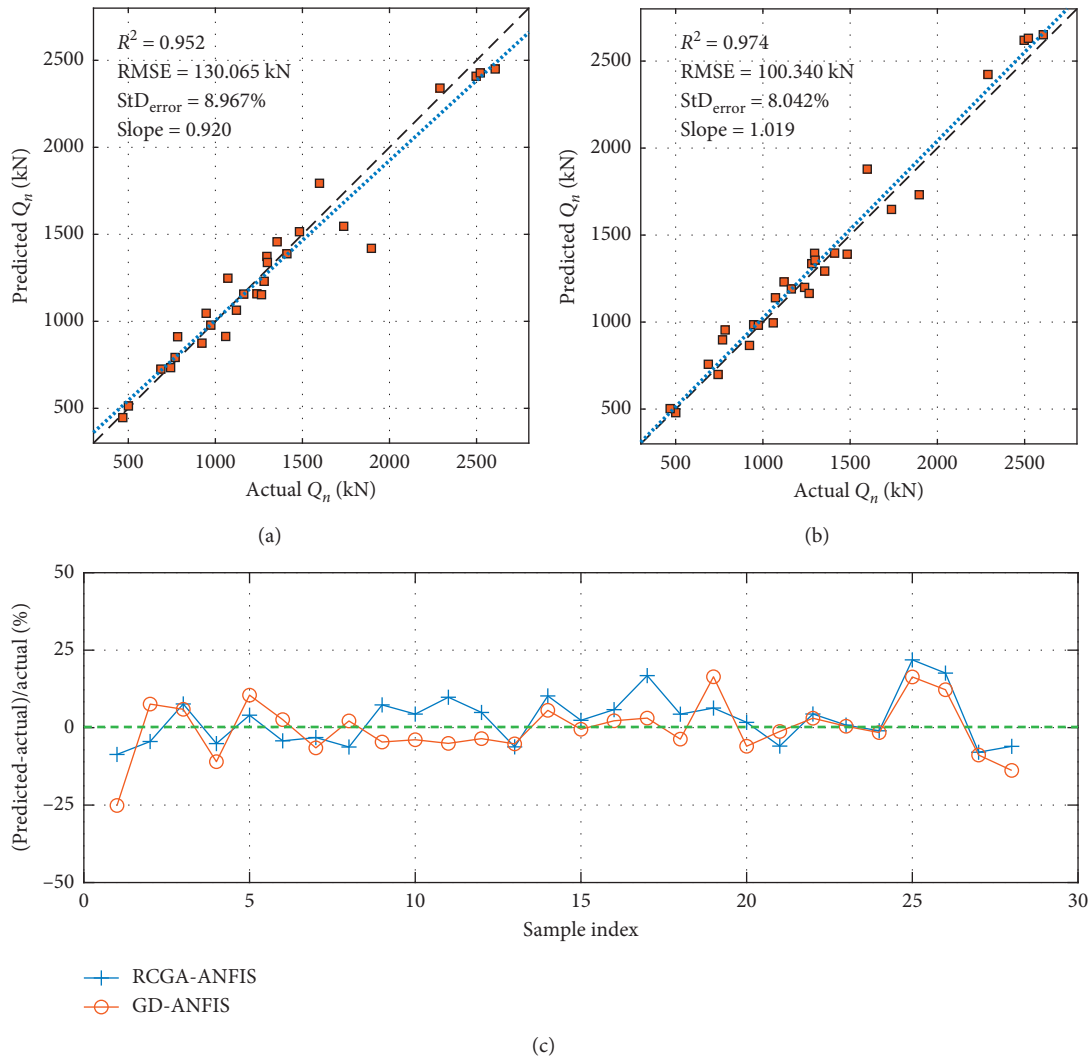

Figure 5: Results after validating process for (a) using GD, (b) using RCGA, and (c) distribution of errors.

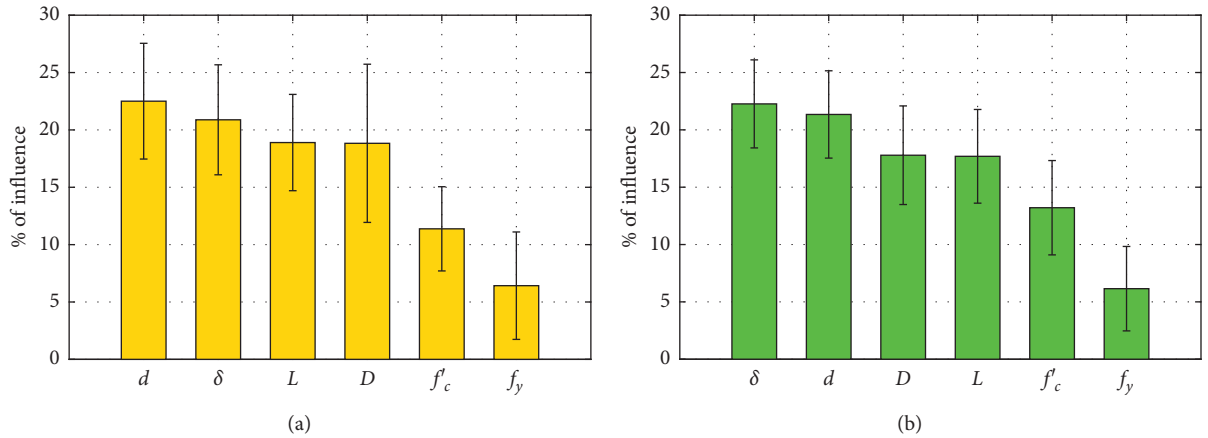

Figure 6: Sensitivity analysis of input variables using (a) GD-ANFIS and (b) RCGA-ANFIS.

Table 5: Statistical analysis of global influence index (in %).

Parameter	Model	L	D	d	δ	f_y	f_c'
Mean	GD-ANFIS	18.898	18.832	22.505	20.882	6.422	11.378
	RCGA-ANFIS	17.692	17.788	21.344	22.264	6.151	13.210
StD	GD-ANFIS	4.198	6.895	5.045	4.795	4.683	3.671
	RCGA-ANFIS	4.085	4.300	3.807	3.839	3.682	4.113

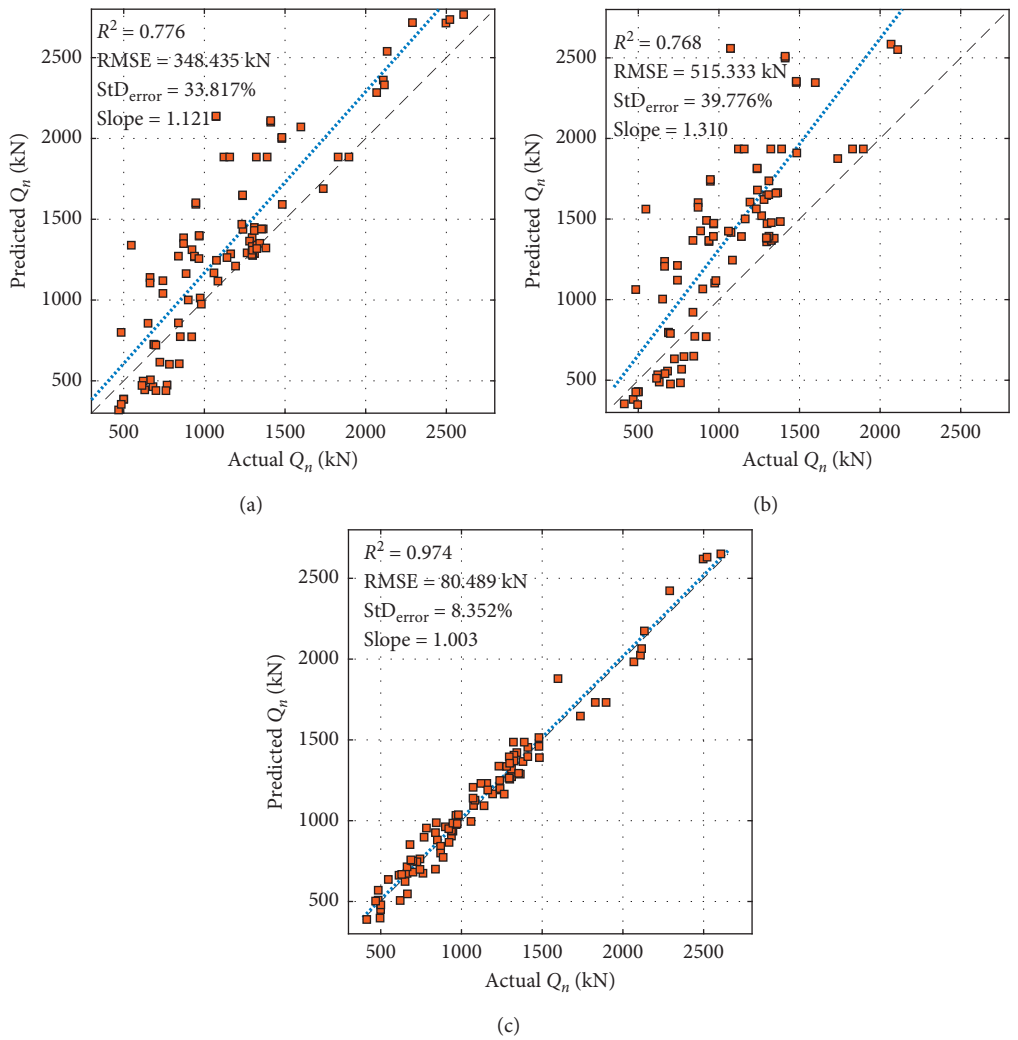

Figure 7: Regression graphs between predicted and actual Q_n (all data) using (a) Liu and Zha [16], (b) Shen et al. [17], and (c) RCGA-ANFIS model.

to all error measurement criteria. In Table 6, the percentage of gain is also indicated. The percentage of gain is calculated based on the following equation:

$$\%\ \text{Gain} = \begin{cases} \left(\left(\Omega^{\text{this-study}} - 1\right) - \left(\Omega^{\text{literature}} - 1\right)\right) \times 100, & \text{in case of: } R^2 \text{ and Slope;} \\ \left(\dfrac{\left(\Omega^{\text{literature}} - \Omega^{\text{this-study}}\right)}{\Omega^{\text{literature}}}\right) \times 100, & \text{in case of: RMSE and ErrorStD.} \end{cases} \tag{14}$$

Table 6: Comparison between RCGA-ANFIS model and literature.

Parameter	Model used	R^2	RMSE	$\text{Mean}_{\text{error}}$	$\text{StD}_{\text{error}}$	Slope	Slope angle (°)
Performance indicator	Liu et al. 2011	0.776	348.435	15.523	33.817	1.121	48.277
	Shen et al. 2015	0.768	515.333	29.887	39.776	1.310	52.636
	This work	0.974	80.489	1.439	8.352	1.003	45.092
% of gain	Liu and Zha [16]	+19.8	+76.9	+90.7	+75.3	+11.8	+7.1
	Shen et al. [17]	+20.6	+84.4	+95.2	+79.0	+30.6	+16.8

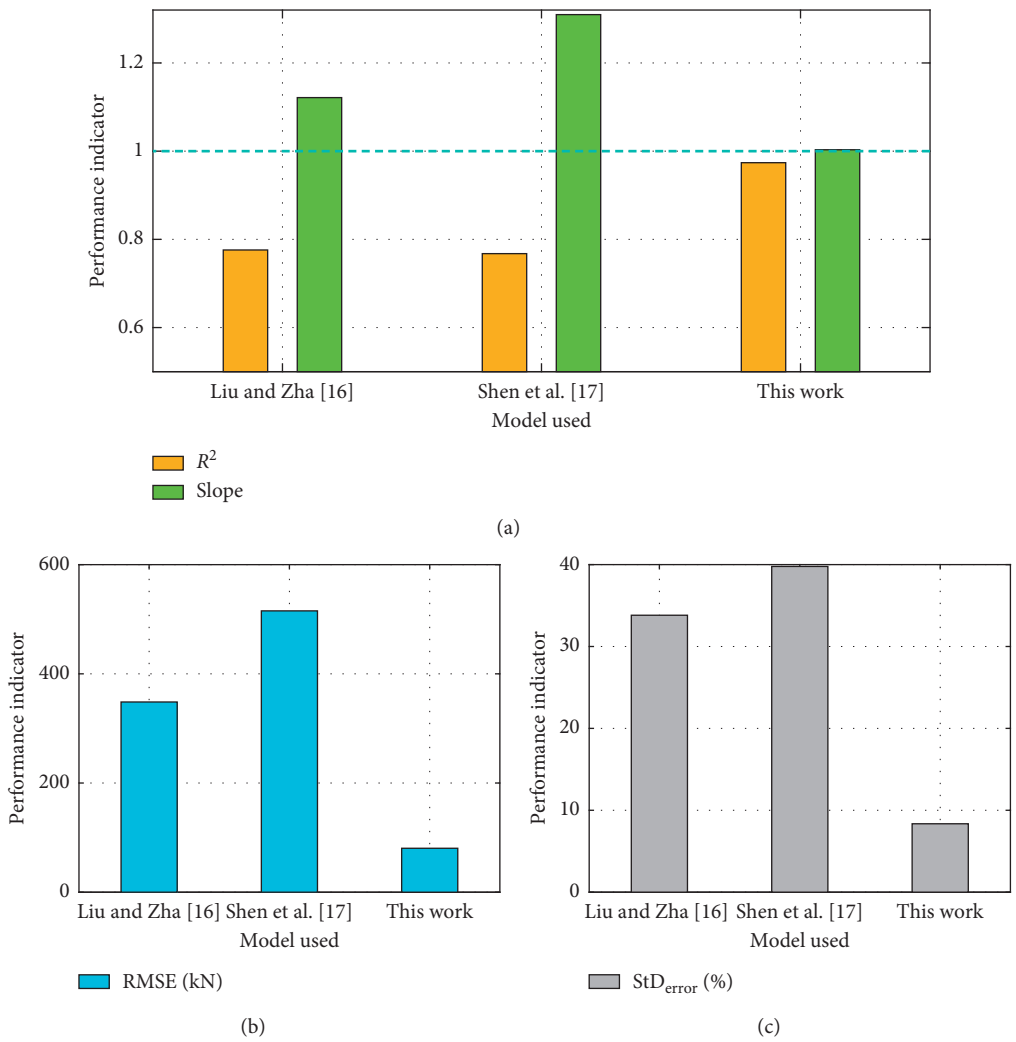

Figure 8: Comparison between RCGA-ANFIS model and literature: (a) in terms of R^2 and slope, (b) in terms of RMSE, and (c) in terms of $\text{StD}_{\text{error}}$.

Figure 8 shows the comparison regarding the performance indicators between RCGA-ANFIS and existing models. Obviously, the RCGA-ANFIS model showed an excellent performance in predicting the ultimate load of the elliptical CFST columns.

3.5. Practical Application. For further application of RCGA-ANFIS model, a Graphical User Interface (GUI) was developed in MATLAB 2018a [73]. Figure 9 presents the main GUI, which is simple and easy to use. Users can enter the values of input variables; the ultimate load of elliptical CFST columns is then displayed directly by clicking the Start Predict button. The GUI is provided freely at https://github.com/Tien-ThinhLe/EllipticalCFST_AxialCapacityPrediction.

3.6. Proposed Empirical Formula. It is not convenient for researchers/engineers to employ machine learning models in practice, because such a model contains weights, bias parameters, and transfer functions. Thus, an empirical formula based on the developed machine learning model should be derived to be employed in the engineering field. Based on the results obtained from the machine learning model, a mathematical method was used to derive a practical

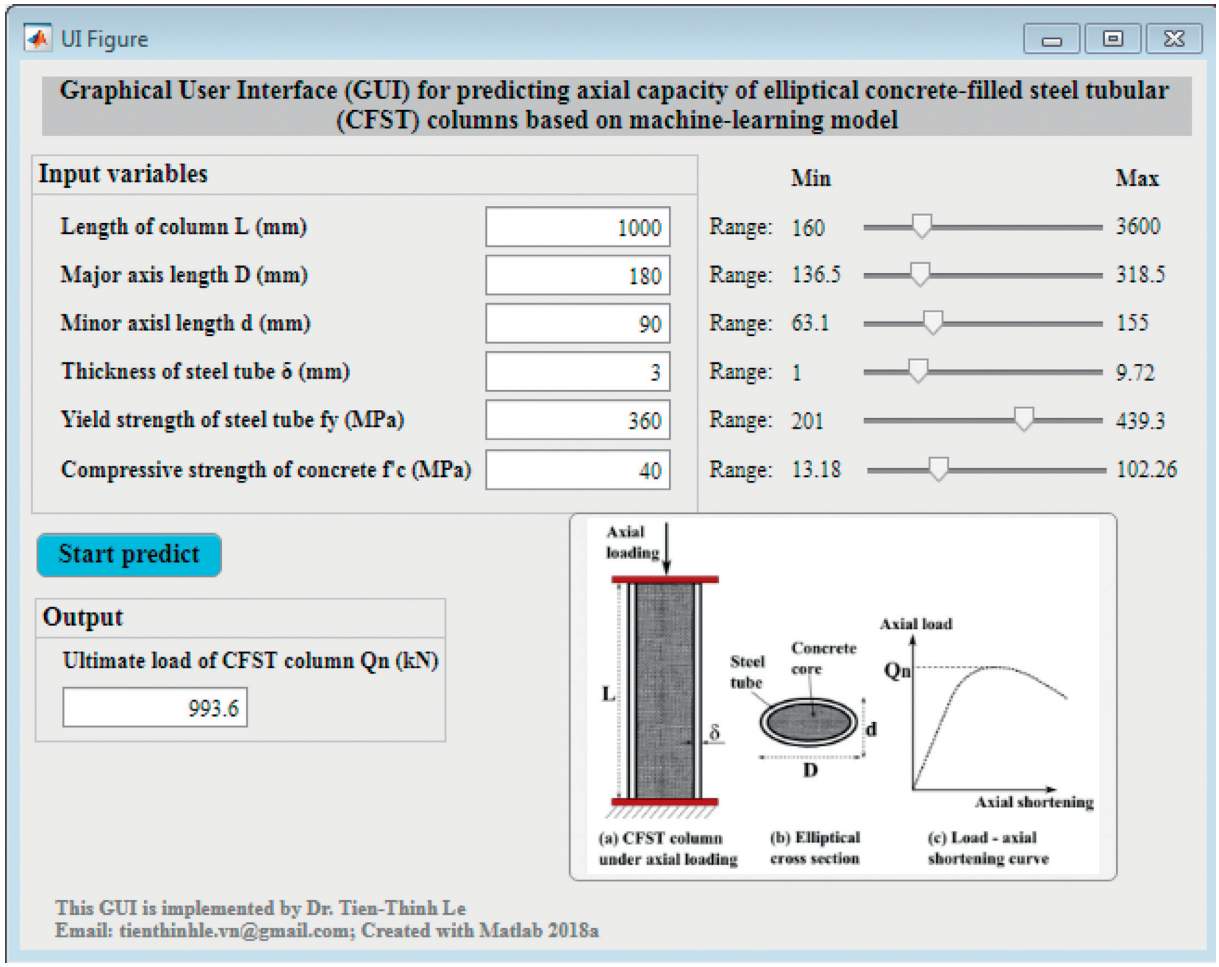

Figure 9: MATLAB's GUI for the prediction of the ultimate load of elliptical CFST columns based on RCGA-ANFIS model.

equation for the prediction of ultimate load of elliptical CFST columns. Such a procedure was inspired by a recent development of Nikbin et al. [74] in deriving an empirical formula for prediction of fracture energy of concrete based on machine learning models. Figure 10 presents the diagram of the procedure. More details could be found in Nikbin et al. [74].

Based on the procedure presented in Figure 10, the ultimate load of elliptical CFST columns can be predicted using

$$Q_n^{\text{Proposed formula}} = C_L \times C_D \times C_d \times C_\delta \times C_{f_y} \times C_{f'_c}, \quad (15)$$

where

$$C_L = -0.0075912 \times \left(\frac{L}{1000}\right)^2 - 0.15675 \times \left(\frac{L}{1000}\right) + 1.2827, \quad (16)$$

$$C_D = -0.25383 \times \left(\frac{D}{180}\right)^2 + 1.313 \times \left(\frac{D}{180}\right) - 0.016222, \quad (17)$$

$$C_d = 0.06122 \times d^2 - 2.7245 \times d + 501.50, \quad (18)$$

$$C_\delta = 0.11857 \times \left(\frac{\delta}{4}\right)^2 + 0.1051 \times \left(\frac{\delta}{4}\right) + 0.83073, \quad (19)$$

$$C_{f_y} = 0.51644 \times \left(\frac{f_y}{350}\right)^2 - 0.70249 \times \left(\frac{f_y}{350}\right) + 1.2644, \quad (20)$$

$$C_{f'_c} = 0.015364 \times \left(\frac{f'_c}{50}\right)^2 + 0.25698 \times \left(\frac{f'_c}{50}\right) + 0.80208. \quad (21)$$

The coefficients presented in (16)–(21) were deduced based on a least square optimization process (see also Nikbin et al. [74]). In order to evaluate the performance of the proposed equation, 94 experimental data points have been employed for a comparison purpose. Details of the experimental dataset, including input variables (geometric variables and strength of constituent materials), output variable (measured ultimate load), and three ratios ($Q_n^{\text{Liu–2011}}/Q_n$), ($Q_n^{\text{Shen–2015}}/Q_n$), ($Q_n^{\text{Proposed formula}}/Q_n$), are indicated in Table 7. At the end of Table 7, statistics of the three ratios are also indicated, including the min, average, max, standard deviation, and coefficient of

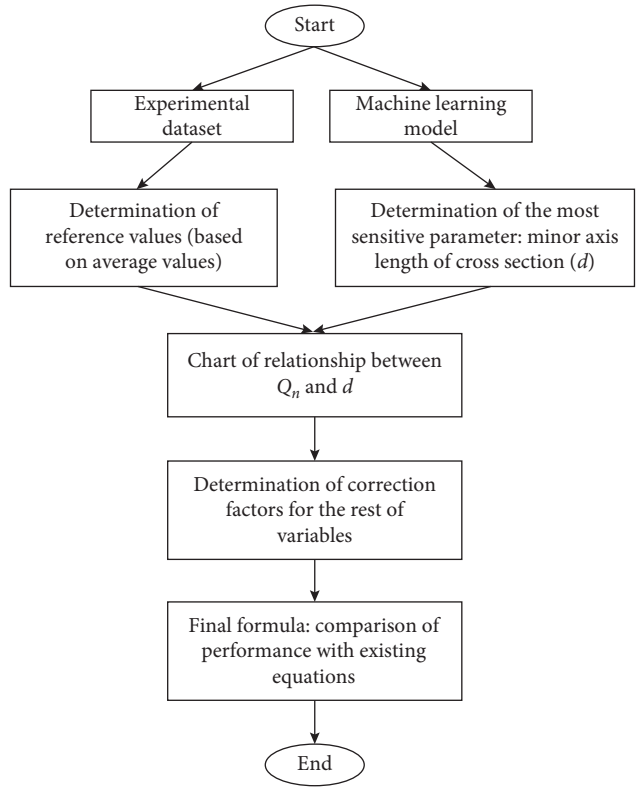

Figure 10: Methodology flowchart for the development of empirical formula.

Table 7: Comparison of performance between the proposed formula and existing equations.

L	D	d	δ	f_y	f_c'	Q_n	$(Q_n^{\text{Liu-2011}}/Q_n)$	$(Q_n^{\text{Shen-2015}}/Q_n)$	$(Q_n^{\text{Proposed formula}}/Q_n)$
mm	mm	mm	mm	MPa	MPa	kN	—	—	—
300	150.4	75.6	4.18	376.5	26.93	839	1.02	1.10	0.96
300	150.57	75.52	4.19	376.5	47.3	974	1.04	1.13	0.93
300	150.39	75.67	4.18	376.5	84.57	1265	1.02	1.20	0.86
300	150.12	75.65	5.12	369	26.93	981	0.99	1.14	0.88
300	150.23	75.74	5.08	369	47.3	1084	1.03	1.15	0.89
300	150.28	75.67	5.09	369	84.57	1296	1.07	1.27	0.90
300	148.78	75.45	6.32	400.5	26.93	1193	1.01	1.35	0.83
300	148.92	75.56	6.43	400.5	47.3	1280	1.07	1.27	0.88
300	149.53	75.35	6.25	400.5	84.57	1483	1.07	1.29	0.90
500	150.18	75.21	4.51	395	69.2	1075	1.16	1.32	0.96
500	150.49	75.26	5.41	358	69.2	1163	1.11	1.29	0.92
500	150.05	75.42	6.56	369	69.2	1310	1.11	1.33	0.92
600	200.21	100.12	5.2	397	69.2	1598	1.30	1.47	1.11
600	200	100.35	6.1	411	69.2	2068	1.10	1.25	0.95
600	200.6	100.02	8.17	383	69.2	2133	1.19	1.41	1.08
600	200.19	100.41	9.72	367	69.2	2290	1.19	1.46	1.15
698	220.7	110.7	6.16	421	48.2	2109	1.12	1.21	1.01
300	150.1	75	4.1	431.4	35.8	900	1.11	1.18	0.99
299	150.1	75.2	4.2	431.4	92.14	1239	1.16	1.36	0.97
398	197.8	100.1	5.1	347.9	36.87	1232	1.19	1.27	1.16
398	197.5	100.2	5.1	347.9	53.54	1737	0.97	1.08	0.90
398	197.4	100.1	5.1	347.9	102.26	2116	1.10	1.35	0.94
1497	150.9	75.4	4	431.4	17.9	650.8	1.32	1.54	1.03
1498	150.4	75.2	4.1	431.4	51.29	742.8	1.51	1.63	1.10
1496	150.3	75.2	4.1	431.4	77	923.2	1.42	1.62	1.01
1499	197.5	100.2	5.2	347.9	20.33	938.4	1.35	1.45	1.18

Table 7: Continued.

L	D	d	δ	f_y	f'_c	Q_n	$(Q_n^{\text{Liu-2011}}/Q_n)$	$(Q_n^{\text{Shen-2015}}/Q_n)$	$(Q_n^{\text{Proposed formula}}/Q_n)$
1498	197.7	100.1	5.1	347.9	77	1480	1.35	1.59	1.01
1785	150.7	75.2	4.2	431.4	51.67	663.2	1.72	1.87	1.18
1786	150.7	75.4	4.1	431.4	86.08	871.2	1.59	1.84	1.06
1785	197.6	100.2	5.1	347.9	31.32	967.5	1.44	1.52	1.15
1786	197.7	100.1	5.1	347.9	50.27	1237	1.33	1.46	1.00
1786	197.3	100	5.2	347.9	83.87	1411.2	1.49	1.77	1.05
2499	197.8	100.1	5.1	347.9	46.2	947	1.68	1.83	1.10
2498	197.7	100.1	5.1	347.9	87.28	1072.3	1.99	2.39	1.20
160	160	107.8	1	207	27.3	768.7	0.62	0.74	1.20
160	159.4	106.5	1.6	296	27.3	844	0.72	0.77	1.12
160	159.7	107.4	2.3	341	27.3	921.3	0.84	0.84	1.12
250	159.9	105.5	1	207	27.3	681.3	0.68	0.82	1.31
250	160.1	105.5	1.6	296	27.3	783.3	0.77	0.83	1.19
250	160.8	107	2.3	341	27.3	850.7	0.91	0.91	1.20
160	159.4	80.5	1.6	279	25	699.7	0.63	0.68	0.99
160	158.8	80.7	2.3	201	25	761.5	0.58	0.64	0.95
250	160.8	74.9	1	211	25	468.4	0.68	0.81	1.35
250	158.3	82	2.3	201	25	630.1	0.71	0.78	1.15
160	159.2	63.2	1	207	27.3	496	0.58	0.70	1.16
160	159.6	63.3	1.6	296	27.3	500.6	0.77	0.86	1.20
160	159.5	64.2	2.3	341	27.3	665.3	0.76	0.81	0.98
250	158.5	64.5	1	207	27.3	413.3	0.71	0.86	1.39
250	159.3	63.1	1.6	296	27.3	499.3	0.77	0.86	1.19
250	158.8	63.2	2.3	341	27.3	620.6	0.80	0.86	1.02
200	158.6	79.7	1	207	27.3	484.6	0.73	0.88	1.38
200	158	80.6	1.6	296	27.3	613.3	0.77	0.84	1.14
200	159.2	82.1	2.3	341	27.3	724	0.85	0.87	1.06
1678	150.4	75.2	4.1	410	45.64	743	1.40	1.51	1.00
1679	197.5	100	5.2	350	20.33	938	1.36	1.46	1.15
1678	197.7	100	5.1	350	77.2	1480	1.36	1.59	0.98
1965	150.5	75.4	4.1	410	13.18	484	1.65	2.20	1.21
1965	150.7	75.2	4.2	410	52.13	663	1.67	1.82	1.11
1966	150.7	75.4	4.1	410	86.18	871	1.55	1.81	1.00
1965	197.6	100	5.1	350	31.32	968	1.45	1.52	1.11
1966	197.7	100	5.1	350	50.27	1237	1.33	1.47	0.97
1966	197.3	100	5.2	350	84.17	1411	1.50	1.78	1.01
2681	150.1	75	4.1	410	86.18	547	2.45	2.86	1.35
2678	197.5	100	5.2	350	20.33	839	1.52	1.63	1.04
2679	197.8	100	5.1	350	46.56	947	1.69	1.84	1.06
2678	197.7	100	5.1	350	87.18	1072	1.99	2.39	1.15
3600	192	124	3.82	439.3	48.41	1121	1.68	1.73	0.89
3600	192	124	3.82	439.3	48.41	1157	1.63	1.67	0.86
2700	192	124	3.82	439.3	48.41	1389	1.36	1.39	0.93
2700	192	124	3.82	439.3	48.41	1322	1.43	1.46	0.98
1800	192	124	3.82	439.3	48.41	1896	0.99	1.02	0.83
1800	192	124	3.82	439.3	48.41	1829	1.03	1.06	0.86
2154	148.45	75.78	6.3	369.1	32	886.6	1.31	1.61	0.82
1154	148.37	75.63	6.3	369.1	33	1059.3	1.10	1.35	0.82
271	136.5	136.5	2.75	376.4	50.36	1296.3	1.03	1.05	1.16
271	137	137	2.75	376.4	50.36	1325.3	1.01	1.03	1.14
271	137.8	137.8	2.75	376.4	50.36	1343	1.01	1.03	1.14
338	170	112	2.75	376.4	50.36	1310.6	0.98	1.06	1.03
338	169.6	111	2.75	376.4	50.36	1299.2	0.98	1.06	1.03
338	168	112.5	2.75	376.4	50.36	1294.4	0.99	1.07	1.04
407	202	99	2.75	376.4	50.36	1298.7	1.01	1.13	1.01
407	199.8	100.8	2.75	376.4	50.36	1325	1.00	1.12	1.01
407	201.5	100.4	2.75	376.4	50.36	1381.1	0.96	1.07	0.97
475	236	95.8	2.75	376.4	50.36	1309.2	1.09	1.26	1.07
475	237.5	96	2.75	376.4	50.36	1364.6	1.06	1.22	1.03
475	236	96.5	2.75	376.4	50.36	1354.2	1.06	1.23	1.04

Table 7: Continued.

L	D	d	δ	f_y	f_c'	Q_n	$(Q_n^{\text{Liu-2011}}/Q_n)$	$(Q_n^{\text{Shen-2015}}/Q_n)$	$(Q_n^{\text{Proposed formula}}/Q_n)$
636	318	155	2.75	376.4	50.36	2607	1.06	1.24	1.21
636	318.5	151.5	2.75	376.4	50.36	2497.3	1.09	1.28	1.22
636	317	153.5	2.75	376.4	50.36	2521.5	1.08	1.27	1.23
279	139	68	2.75	376.4	50.36	687.2	1.06	1.16	1.04
279	138	68.2	2.75	376.4	50.36	688.1	1.05	1.15	1.04
279	137.5	68	2.75	376.4	50.36	699.2	1.03	1.13	1.02
2670.4	199.7	105.7	2.6	376.4	45	1140	1.11	1.22	0.79
1910.4	204.3	103.1	2.6	376.4	45	966	1.30	1.44	1.09
						Min	0.58	0.64	0.79
						Average	1.16	1.30	1.05
						Max	2.45	2.86	1.39
						StD*	0.34	0.40	0.13
						CV**	29.27	30.62	12.55

StD: standard deviation, CV: coefficient of variation (%).

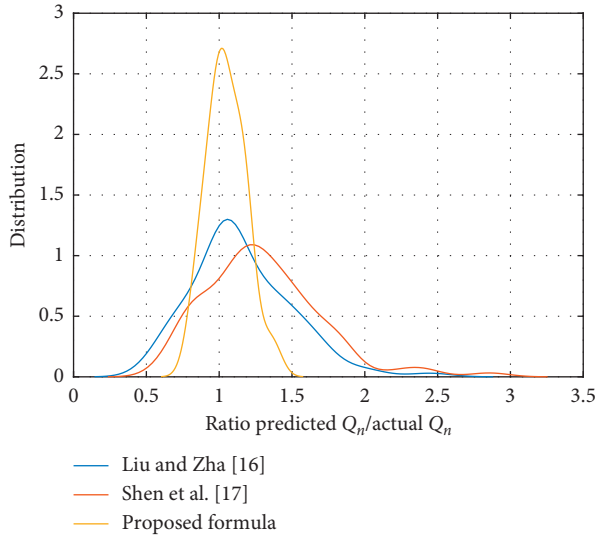

Figure 11: Distribution of ratio predicted Q_n/actual Q_n using different equations.

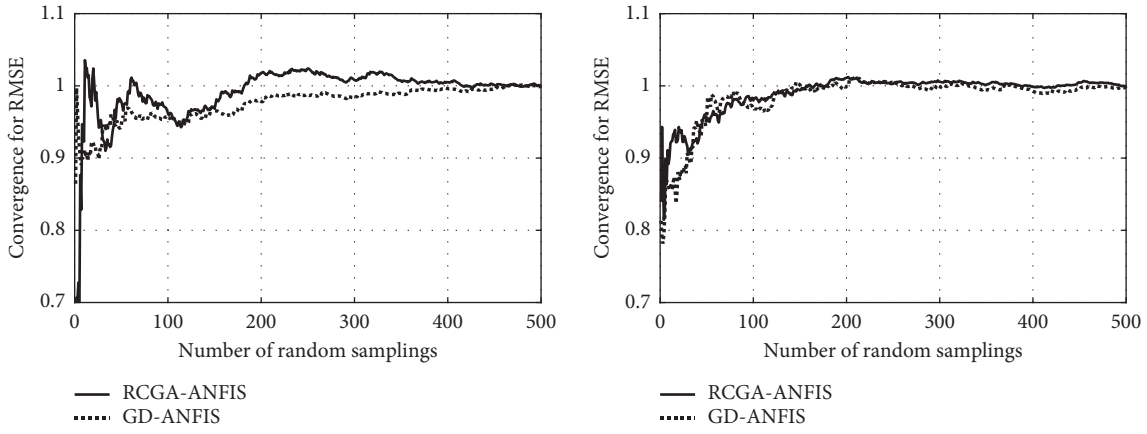

Figure 12: Continued.

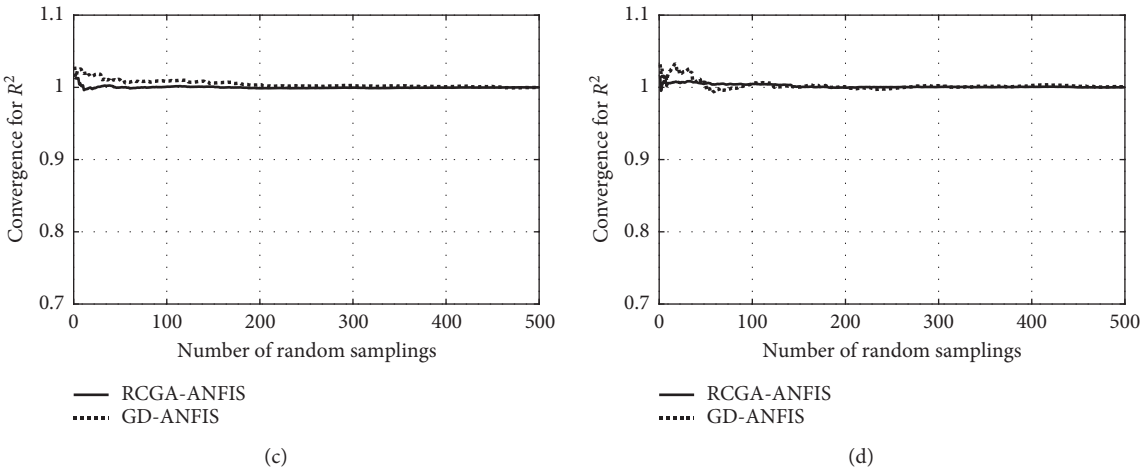

Figure 12: Monte Carlo convergence for training data: (a) RMSE, (b) R^2; for testing data: (c) RMSE, (d) R^2.

variation values. Finally, Figure 11 shows the probability density distribution of the three ratios.

It is seen in Table 7 (statistics of the three ratios) and Figure 11 that the prediction based on the proposed formula exhibits the highest agreement with the experimental data points or, in other words, the lowest error measurements (an average value of 1.05 compared to 1.16, 1.30 using Liu and Shen equations; a standard deviation value of 0.13 compared to 0.34, 0.40 using Liu and Shen equations; and a coefficient of variation of 12.55% compared to 29.27, 30.62 using Liu and Shen equations, respectively). It can be concluded that the prediction performance based on the proposed formula is superior to those available in the literature. Thus, with a simple form, the proposed formula can be used in practice. Moreover, if more experimental data are available in the future, the model will be improved (i.e., for a wider range of data).

4. Conclusions

The research presented in this article proposed a robust surrogate tool for the estimation of the ultimate load of elliptical CFST members under axial compression. Based on the developments and analyses, the following conclusions may be made:

(i) An experimental dataset was collected from the available literature for the development of the models including two groups of variables: geometric dimensions of cross section and mechanical properties of constituent materials (concrete and steel).

(ii) Two hybrid ML models, namely, the conventional GD-ANFIS and metaheuristic-based RCGA-ANFIS, were proposed to predict the ultimate load of the columns. The results showed that the RCGA-ANFIS model outperformed GD-ANFIS. In addition, the performance of the RCGA-ANFIS model was superior to two empirical equations in the literature.

(iii) The robustness of the proposed models was assessed by conducting Monte Carlo simulations taking into account the variability in the input space.

(iv) Sensitivity analysis showed that the steel pipe wall thickness and the short side length of the cross section were the most critical parameters affecting the bearing capacity of elliptical CFST columns (i.e., 22.264% and 21.344%, respectively).

(v) A Graphical User Interface was developed and provided freely for researchers/engineers/interested users. The results of the present work could simplify the design of elliptical CFST columns. The optimum values obtained in this study could allow quick and accurate determining of the bearing capacity of elliptical CFST columns for practical purposes.

However, it is worth noticing that, in this research, only elliptical CFST columns were considered. It is well-known that the cross section of columns has other forms; thus, the extension of the GUI to other cross sections would be the main perspective of the next study. In further research, a generic model should be developed for different types of cross section (i.e., circular, rectangular, square, hexagonal, etc.). Such a model can be highly beneficial for the research and practical purposes. Finally, in terms of practical application, a GUI based on Excel should be developed for wider applicability.

Appendix

Convergence of Monte Carlo simulations

In this section, the convergence of the ML models in the function of Monte Carlo runs is investigated (see Section 2.2.3). Figure 12 shows the convergence estimation in terms of RMSE and R^2, using the training and testing data, respectively. Regarding the convergence of R^2 for both training and testing part, low order of fluctuation was observed compared to RMSE. The statistical convergence analyses

showed that at least 500 Monte Carlo simulations were needed to obtain reliable results, particularly in terms of RMSE.

Data Availability

The Excel format data used to support the findings of this study may be made available upon request to Dr. Tien-Thinh Le, who can be contacted via thinh.letien@phenikaa-uni.edu.vn.

Conflicts of Interest

The author declares that there are no conflicts of interest regarding the publication of this paper.

Acknowledgments

The author would like to thank Prof. Lu Minh Le (Vietnam National University of Agriculture, Vietnam), Dr. Hai-Bang Ly, Dr. Binh Thai Pham, and Dr. Thuy Anh Nguyen (University of Transport Technology, Vietnam) for their helpful advice and comments on this paper.

References

[1] J. Yang, T. Sheehan, X. H. Dai, and D. Lam, "Experimental study of beam to concrete-filled elliptical steel tubular column connections," *Thin-Walled Structures*, vol. 95, pp. 16–23, 2015.

[2] F. McCann, "Concrete-filled elliptical section steel columns under concentric and eccentric loading," in *Proceedings of the 8th International Conference on Advances in Steel Structures, 2015*, Lisbon, Portugal, 2015.

[3] A. Espinos, L. Gardner, M. L. Romero, and A. Hospitaler, "Fire behaviour of concrete filled elliptical steel columns," *Thin-Walled Structures*, vol. 49, no. 2, pp. 239–255, 2011.

[4] S.-H. Lee, B. Uy, S.-H. Kim, Y.-H. Choi, and S.-M. Choi, "Behavior of high-strength circular concrete-filled steel tubular (CFST) column under eccentric loading," *Journal of Constructional Steel Research*, vol. 67, no. 1, pp. 1–13, 2011.

[5] T.-T. Le, "Surrogate neural network model for prediction of load-bearing capacity of CFSS members considering loading eccentricity," *Applied Sciences*, vol. 10, no. 10, p. 3452, 2020.

[6] H. Thanh Duong, H. Chi Phan, T.-T. Le, and N. Duc Bui, "Optimization design of rectangular concrete-filled steel tube short columns with balancing composite motion optimization and data-driven model," *Structures*, vol. 28, pp. 757–765, 2020.

[7] F. Ding, X. Ding, X. Liu, H. Wang, Z. Yu, and C. Fang, "Mechanical behavior of elliptical concrete-filled steel tubular stub columns under axial loading," *Steel and Composite Structures*, vol. 25, no. 3, pp. 375–388, 2017.

[8] H.-B. Ly, B. T. Pham, L. M. Le, T.-T. Le, V. M. Le, and P. G. Asteris, "Estimation of axial load-carrying capacity of concrete-filled steel tubes using surrogate models," *Neural Computing and Applications*, 2020, In press.

[9] L. Dennis and T. Nicola, "Structural design of concrete filled steel elliptical hollow sections," *Composite Construction in Steel and Concrete VI*, American Society of Civil Engineers, Reston, VA, USA, 2008.

[10] Y. Xu, J. Yao, and X. Sun, "Cold-formed elliptical concrete-filled steel tubular columns subjected to monotonic and cyclic axial compression," *Advances in Structural Engineering*, vol. 23, no. 7, p. 1383, 2019.

[11] T. M. Chan, L. Gardner, and K. H. Law, "Structural design of elliptical hollow sections: a review," *Proceedings of the Institution of Civil Engineers—Structures and Buildings*, vol. 163, no. 6, pp. 391–402, 2010.

[12] Q.-X. Ren, L.-H. Han, D. Lam, and W. Li, "Tests on elliptical concrete filled steel tubular (CFST) beams and columns," *Journal of Constructional Steel Research*, vol. 99, pp. 149–160, 2014.

[13] V. Q. Tran, H. L. Nguyen, V. D. Dao et al., "Effect of temperature on the chloride binding capacity of cementitious materials," *Magazine of Concrete Research*, pp. 1–39, 2019, In press.

[14] F. McCann and L. Gardner, "Numerical analysis and design of slender elliptical hollow sections in bending," *Thin-Walled Structures*, vol. 139, pp. 196–208, 2019.

[15] Y. Xu and J. Yao, "Axial bearing capacity of elliptical concrete filled steel tubular stub columns," *IOP Conference Series: Materials Science and Engineering*, vol. 220, Article ID 012002, 2017.

[16] X. C. Liu and X. X. Zha, "Study on behavior of elliptical concrete filled steel tube members I: stub and long columns under axial compression," *Progress in Steel Building Structures*, vol. 1, pp. 8–14, 2011.

[17] Q. H. Shen, J. F. Wang, W. Wang, and J. Wang, "Axial compressive behavior and bearing capacity calculation of ECFST columns based on numerical analysis," *Progress in Steel Building Structures*, vol. 6, pp. 68–78, 2015.

[18] Q. H. Nguyen, H.-B. Ly, T.-T. Le et al., "Parametric investigation of particle swarm optimization to improve the performance of the adaptive neuro-fuzzy inference system in determining the buckling capacity of circular opening steel beams," *Materials*, vol. 13, no. 10, p. 2210, 2020.

[19] H.-B. Ly, T.-T. Le, H.-L. T. Vu, V. Q. Tran, L. M. Le, and B. T. Pham, "Computational hybrid machine learning based prediction of shear capacity for steel fiber reinforced concrete beams," *Sustainability*, vol. 12, no. 7, p. 2709, 2020.

[20] H. Q. Nguyen, H.-B. Ly, V. Q. Tran, T.-A. Nguyen, T.-T. Le, and B. T. Pham, "Optimization of artificial intelligence system by evolutionary algorithm for prediction of axial capacity of rectangular concrete filled steel tubes under compression," *Materials*, vol. 13, no. 5, p. 1205, 2020.

[21] Q. H. Nguyen, H.-B. Ly, V. Q. Tran et al., "A novel hybrid model based on a feedforward neural network and one step secant algorithm for prediction of load-bearing capacity of rectangular concrete-filled steel tube columns," *Molecules*, vol. 25, no. 15, p. 3486, 2020.

[22] P. Sarir, J. Chen, P. G. Asteris, D. J. Armaghani, and M. M. Tahir, "Developing GEP tree-based, neuro-swarm, and whale optimization models for evaluation of bearing capacity of concrete-filled steel tube columns," *Engineering with Computers*, 2019, In press.

[23] M. Ahmadi, H. Naderpour, and A. Kheyroddin, "Utilization of artificial neural networks to prediction of the capacity of CCFT short columns subject to short term axial load," *Archives of Civil and Mechanical Engineering*, vol. 14, no. 3, pp. 510–517, 2014.

[24] M. Ahmadi, H. Naderpour, and A. Kheyroddin, "ANN model for predicting the compressive strength of circular steel-confined concrete," *International Journal of Civil Engineering*, vol. 15, no. 2, pp. 213–221, 2017.

[25] V.-L. Tran, D.-K. Thai, and S.-E. Kim, "Application of ANN in predicting ACC of SCFST column," *Composite Structures*, vol. 228, Article ID 111332, 2019.

[26] E. M. Güneyisi, A. Gültekin, and K. Mermerdaş, "Ultimate capacity prediction of axially loaded CFST short columns," *International Journal of Steel Structures*, vol. 16, no. 1, pp. 99–114, 2016.

[27] J. Moon, J. J. Kim, T.-H. Lee, and H.-E. Lee, "Prediction of axial load capacity of stub circular concrete-filled steel tube using fuzzy logic," *Journal of Constructional Steel Research*, vol. 101, pp. 184–191, 2014.

[28] K. Uenaka, "Experimental study on concrete filled elliptical/oval steel tubular stub columns under compression," *Thin-Walled Structures*, vol. 78, pp. 131–137, 2014.

[29] H. Yang, F. Liu, T.-m. Chan, and W. Wang, "Behaviours of concrete-filled cold-formed elliptical hollow section beam-columns with varying aspect ratios," *Thin-Walled Structures*, vol. 120, pp. 9–28, 2017.

[30] F. Liu, Y. Wang, and T.-m. Chan, "Behaviour of concrete-filled cold-formed elliptical hollow sections with varying aspect ratios," *Thin-Walled Structures*, vol. 110, pp. 47–61, 2017.

[31] X. H. Dai, D. Lam, N. Jamaluddin, and J. Ye, "Numerical analysis of slender elliptical concrete filled columns under axial compression," *Thin-Walled Structures*, vol. 77, pp. 26–35, 2014.

[32] N. Jamaluddin, D. Lam, X. H. Dai, and J. Ye, "An experimental study on elliptical concrete filled columns under axial compression," *Journal of Constructional Steel Research*, vol. 87, pp. 6–16, 2013.

[33] H. Yang, D. Lam, and L. Gardner, "Testing and analysis of concrete-filled elliptical hollow sections," *Engineering Structures*, vol. 30, no. 12, pp. 3771–3781, 2008.

[34] F. McCann, L. Gardner, and W. Qiu, "Experimental study of slender concrete-filled elliptical hollow section beam-columns," *Journal of Constructional Steel Research*, vol. 113, pp. 185–194, 2015.

[35] X. L. Zhao and J. A. Packer, "Tests and design of concrete-filled elliptical hollow section stub columns," *Thin-Walled Structures*, vol. 47, no. 6-7, pp. 617–628, 2009.

[36] I. T. Jolliffe, *Principal Component Analysis*, Springer-Verlag, New York, NY, USA, 2nd edition, 2002.

[37] J.-S. R. Jang, "ANFIS: adaptive-network-based fuzzy inference system," *IEEE Transactions on Systems, Man, and Cybernetics*, vol. 23, no. 3, p. 665, 1993.

[38] J.-S. R. Jang, C.-T. Sun, and E. Mizutani, *Neuro-Fuzzy and Soft Computing: A Computational Approach to Learning and Machine Intelligence*, Prentice-Hall, Upper Saddle River, NJ, USA, 1997.

[39] M. Bilgehan, "Comparison of ANFIS and NN models—with a study in critical buckling load estimation," *Applied Soft Computing*, vol. 11, no. 4, pp. 3779–3791, 2011.

[40] H.-L. Nguyen, B. T. Pham, L. H. Son et al., "Adaptive network based fuzzy inference system with meta-heuristic optimizations for international roughness index prediction," *Applied Sciences*, vol. 9, no. 21, p. 4715, 2019.

[41] H.-L. Nguyen, T.-H. Le, C.-T. Pham et al., "Development of hybrid artificial intelligence approaches and a support vector machine algorithm for predicting the marshall parameters of stone matrix asphalt," *Applied Sciences*, vol. 9, no. 15, p. 3172, 2019.

[42] H.-B. Ly, L. M. Le, L. V. Phi et al., "Development of an AI model to measure traffic air pollution from multisensor and weather data," *Sensors*, vol. 19, no. 22, p. 4941, 2019.

[43] H.-B. Ly, L. M. Le, H. T. Duong et al., "Hybrid artificial intelligence approaches for predicting critical buckling load of structural members under compression considering the influence of initial geometric imperfections," *Applied Sciences*, vol. 9, no. 11, p. 2258, 2019.

[44] D. Dao, H.-B. Ly, S. Trinh, T.-T. Le, and B. Pham, "Artificial intelligence approaches for prediction of compressive strength of geopolymer concrete," *Materials*, vol. 12, no. 6, p. 983, 2019.

[45] J. Holland, *Adaptation in Natural and Artificial Systems*, University of Michigan Press, Ann Arbor, MI, USA, 1975.

[46] M. Mitchell, *An Introduction to Genentic Algorithms*, MIT Press, Cambridge, MA, USA, 1998.

[47] D. Whitley, "A genetic algorithm tutorial," *Statistics and Computing*, vol. 4, pp. 65–85, 1994.

[48] W. Wan and J. B. Birch, "An improved hybrid genetic algorithm with a new local search procedure," *Journal of Applied Mathematics*, vol. 2013, Article ID 103591, 10 pages, 2013.

[49] H.-F. Wang and K.-Y. Wu, "Hybrid genetic algorithm for optimization problems with permutation property," *Computers & Operations Research*, vol. 31, no. 14, pp. 2453–2471, 2004.

[50] H.-j. Kim and K.-s. Shin, "A hybrid approach based on neural networks and genetic algorithms for detecting temporal patterns in stock markets," *Applied Soft Computing*, vol. 7, no. 2, pp. 569–576, 2007.

[51] L. M. Le, H.-B. Ly, B. T. Pham et al., "Hybrid artificial intelligence approaches for predicting buckling damage of steel columns under axial compression," *Materials*, vol. 12, no. 10, p. 1670, 2019.

[52] X. Yan, H. Liu, Z. Zhu, and Q. Wu, "Hybrid genetic algorithm for engineering design problems," *Cluster Computing*, vol. 20, no. 1, pp. 263–275, 2017.

[53] C. K. H. Lee, "A review of applications of genetic algorithms in operations management," *Engineering Applications of Artificial Intelligence*, vol. 76, pp. 1–12, 2018.

[54] B. Staber, J. Guilleminot, C. Soize, J. Michopoulos, and A. Iliopoulos, "Stochastic modeling and identification of a hyperelastic constitutive model for laminated composites," *Computer Methods in Applied Mechanics and Engineering*, vol. 347, pp. 425–444, 2019.

[55] T. T. Le, J. Guilleminot, and C. Soize, "Stochastic continuum modeling of random interphases from atomistic simulations. Application to a polymer nanocomposite," *Computer Methods in Applied Mechanics and Engineering*, vol. 303, pp. 430–449, 2016.

[56] J. Guilleminot, T. T. Le, and C. Soize, "Stochastic framework for modeling the linear apparent behavior of complex materials: application to random porous materials with interphases," *Acta Mechanica Sinica*, vol. 29, no. 6, pp. 773–782, 2013.

[57] H.-B. Ly, E. Monteiro, T.-T. Le et al., "Prediction and sensitivity analysis of bubble dissolution time in 3D selective laser sintering using ensemble decision trees," *Materials*, vol. 12, no. 9, p. 1544, 2019.

[58] J. Guilleminot and C. Soize, "Stochastic model and generator for random fields with symmetry properties: application to the mesoscopic modeling of elastic random media," *Multiscale Modeling & Simulation*, vol. 11, no. 3, pp. 840–870, 2013.

[59] D. A. Hun, J. Guilleminot, J. Yvonnet, and M. Bornert, "Stochastic multiscale modeling of crack propagation in random heterogeneous media," *International Journal for*

Numerical Methods in Engineering, vol. 119, no. 13, pp. 1325–1344, 2019.

[60] S. Chu and J. Guilleminot, "Stochastic multiscale modeling with random fields of material properties defined on non-convex domains," *Mechanics Research Communications*, vol. 97, pp. 39–45, 2019.

[61] T.-T. Le, *Modélisation stochastique, en mécanique des milieux continus, de l'interphase inclusion-matrice à partir de simulations en dynamique moléculaire*, Ph.D. thesis, University of Paris-Est Marne-la-Vallée, Paris, France, 2015.

[62] D. V. Dao, H. Adeli, H.-B. Ly et al., "A sensitivity and robustness analysis of GPR and ANN for high-performance concrete compressive strength prediction using a Monte Carlo simulation," *Sustainability*, vol. 12, no. 3, p. 830, 2020.

[63] T.-T. Le, "Probabilistic investigation of the effect of stochastic imperfect interfaces in nanocomposites," *Mechanics of Materials*, vol. 151, Article ID 103608, 2020.

[64] B. Staber and J. Guilleminot, "Stochastic modeling of a class of stored energy functions for incompressible hyperelastic materials with uncertainties," *Comptes Rendus Mécanique*, vol. 343, no. 9, pp. 503–514, 2015.

[65] J. Guilleminot and J. E. Dolbow, "Data-driven enhancement of fracture paths in random composites," *Mechanics Research Communications*, vol. 103, Article ID 103443, 2020.

[66] D. V. Dao, H.-B. Ly, H.-L. T. Vu, T.-T. Le, and B. T. Pham, "Investigation and optimization of the C-ANN structure in predicting the compressive strength of foamed concrete," *Materials*, vol. 13, no. 5, p. 1072, 2020.

[67] B. T. Pham, T. Nguyen-Thoi, H.-B. Ly et al., "Extreme learning machine based prediction of soil shear strength: a sensitivity analysis using Monte Carlo simulations and feature backward elimination," *Sustainability*, vol. 12, no. 6, p. 2339, 2020.

[68] H.-B. Ly, T.-T. Le, L. M. Le et al., "Development of hybrid machine learning models for predicting the critical buckling load of I-shaped cellular beams," *Applied Sciences*, vol. 9, no. 24, p. 5458, 2019.

[69] T.-T. Le, "Probabilistic modeling of surface effects in nano-reinforced materials," *Computational Materials Science*, vol. 186, Article ID 109987, 2021.

[70] T.-T. Le, "Prediction of tensile strength of polymer carbon nanotube composites using practical machine learning method," *Journal of Composite Materials*, 2020, In press.

[71] İ1 Güler and E. D. Übeyli, "Adaptive neuro-fuzzy inference system for classification of EEG signals using wavelet coefficients," *Journal of Neuroscience Methods*, vol. 148, no. 2, pp. 113–121, 2005.

[72] A. F. Mashaly and A. A. Alazba, "ANFIS modeling and sensitivity analysis for estimating solar still productivity using measured operational and meteorological parameters," *Water Supply*, vol. 18, no. 4, pp. 1437–1448, 2018.

[73] MATLAB, *The MathWorks*, MATLAB, Natick, MA, USA, 2018.

[74] I. M. Nikbin, S. Rahimi, and H. Allahyari, "A new empirical formula for prediction of fracture energy of concrete based on the artificial neural network," *Engineering Fracture Mechanics*, vol. 186, pp. 466–482, 2017.